

# Momentum and Asymmetry Spectrum of $\mu$ -Meson Decay\*

RICHARD J. PLANO

Columbia University, New York, New York

(Received April 8, 1960)

The beta decay of the positive  $\mu$  meson was studied using a liquid hydrogen bubble chamber in a magnetic field of 8800 gauss. An analysis of 9213 events used in the momentum spectrum yielded  $\rho=0.780\pm0.025$ . This number includes the internal radiative corrections and is to be compared directly with the 0.75 predicted by two component theory. The analysis of 8354 events used in the asymmetry spectrum gave for the magnitude of the asymmetry  $|\xi|=0.94\pm0.07$  and for the shape parameter  $\delta=0.78\pm0.05$ .

## I. INTRODUCTION

THE investigation of the decay of the  $\mu$  meson received a large impetus through the discovery of nonconservation of parity<sup>1-4</sup> and the successes of the two-component theory of the neutrino<sup>5-7</sup> and the "universal"  $V-A$  theory.<sup>8-10</sup>  $\mu$ -meson decay is especially useful as a check on the exactitude of these theories since no strongly interacting particles participate, so that the only correction is due to the well-understood electromagnetic forces.

In the general four component case, the momentum<sup>11</sup> and asymmetry<sup>12</sup> spectrum including radiative corrections<sup>13,14</sup> is given by:

$$P(x, \cos\theta)dx d(\cos\theta) = \frac{1}{2} \left\{ \frac{1+h(x)}{1+4(m_e/m_\mu)\eta} \left[ 12x^2 - 12x^3 + \rho \left( \frac{32}{3}x^3 - 8x^2 \right) + 24 \frac{m_e}{m_\mu} x(1-x)\eta \right] - \bar{P}\xi \cos\theta \left[ 4x^2 - 4x^3 + \delta \left( \frac{32}{3}x^3 - 8x^2 \right) + \frac{\alpha}{2\pi} g(x) \right] \right\} dx d(\cos\theta). \quad (1)$$

Here,  $x$  is the electron momentum in units of the maxi-

mum possible momentum,  $m_e$  and  $m_\mu$  are the electron and muon masses,  $\bar{P}$  is the average polarization of the muon sample,  $h(x)$  and  $g(x)$  describe the radiative corrections, and  $\theta$  is the angle between the muon and electron momenta. The four parameters  $\rho$ ,  $\xi$ ,  $\delta$ , and  $\eta$  are bilinear functions of the five possible coupling constants and completely specify the shape of the spectrum. Three of these four parameters were evaluated in this experiment. The fourth,  $\eta$ , produces, at most, a very small effect on the shape of the spectrum and could not be determined due to insufficient statistical and systematic accuracy.

This experiment was done in a liquid hydrogen bubble chamber 12 in. in diameter by 6 in. deep in a magnetic field of about 8800 gauss. The beam was adjusted so that 10-15 positive pions stopped in the chamber in each picture. A typical picture is shown in Fig. 1.

The muons from the decay of these stopped pions were 100% polarized along the direction of their momentum according to two component theory. This polarization was partly destroyed by the magnetic field, but the component along the magnetic field was not altered by the field. This fact made it possible to accurately measure the polarization of the sample assuming that the muons were emitted completely polarized and that they were not depolarized by the liquid hydrogen.

Early work on the momentum spectrum showed considerable disparity due to underestimation of systematic errors, particularly in the muon mass. More recent determinations are in considerably better agreement with each other, but most experiments<sup>15-17</sup> indicate a  $\rho$  value somewhat below the value (0.75) predicted by two-component theory.

The asymmetry integrated over all or a large part of spectrum has been measured by a large number of workers with counters,<sup>3,18,19</sup> emulsion,<sup>4,20,21</sup> and a liquid hydrogen bubble chamber.<sup>22</sup>

<sup>15</sup>  $\rho=0.67\pm0.05$ : L. Rosenson, Phys. Rev. **109**, 958 (1958). This report contains extensive references to earlier work.

<sup>16</sup>  $\rho=0.68\pm0.02$ : K. E. Crowe (unpublished).

<sup>17</sup>  $\rho=0.741\pm0.022$ : W. F. Dudziak, R. Sagane, and J. Vedder, Phys. Rev. **114**, 336 (1959).

<sup>18</sup> M. Bardon, D. Berley, and L. M. Lederman, Phys. Rev. Letters **2**, 56 (1959).

<sup>19</sup> Robert A. Swanson, Phys. Rev. **112**, 580 (1958).

<sup>20</sup> S. A. Ali-Zade, I. I. Gurevich, U. P. Dobretsov, B. A. Nikol'ski, and L. V. Surkova, J. Exptl. Theoret. Physics (U.S.S.R.)

\* This research is supported by the U. S. Atomic Energy Commission and the Office of Naval Research.

<sup>1</sup> T. D. Lee and C. N. Yang, Phys. Rev. **104**, 254 (1956).

<sup>2</sup> C. S. Wu, E. Ambler, R. W. Hayward, D. D. Hoppes, and R. P. Hudson, Phys. Rev. **105**, 1413 (1957).

<sup>3</sup> R. Garwin, L. M. Lederman, and M. Weinrich, Phys. Rev. **105**, 1415 (1957).

<sup>4</sup> J. I. Friedman and V. L. Telegdi, Phys. Rev. **106**, 1290 (1957).

<sup>5</sup> T. D. Lee and C. N. Yang, Phys. Rev. **105**, 1671 (1957).

<sup>6</sup> A. Salam, Nuovo cimento **5**, 299 (1957).

<sup>7</sup> L. Landau, Nuclear Phys. **3**, 127 (1957).

<sup>8</sup> R. P. Feynman and M. Gell-Mann, Phys. Rev. **109**, 193 (1958).

<sup>9</sup> E. C. G. Sudarshan and R. E. Marshak, Phys. Rev. **109**, 1860 (1958).

<sup>10</sup> J. J. Sakurai, Nuovo cimento **7**, 649 (1958).

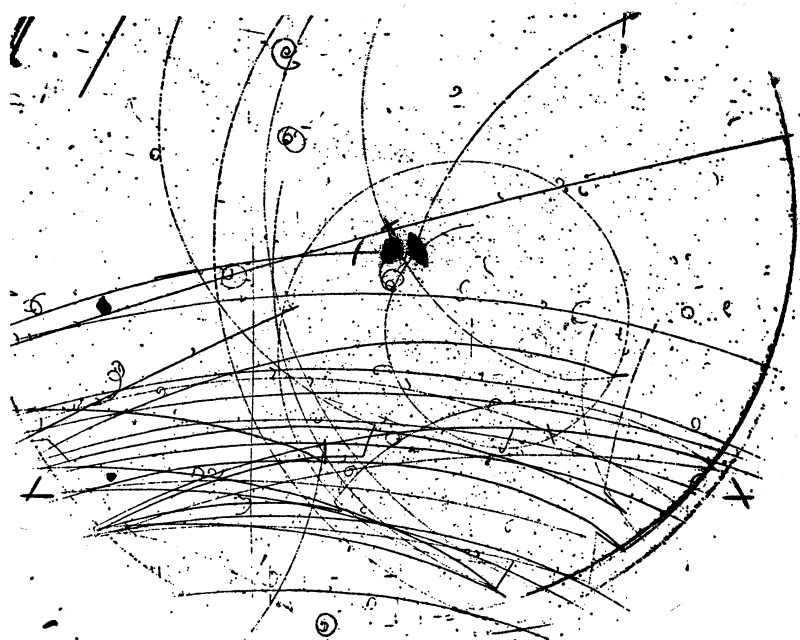
<sup>11</sup> L. Michel, Proc. Phys. Soc. (London) **A63**, 514 (1950).

<sup>12</sup> C. Bouchiat and L. Michel, Phys. Rev. **106**, 170 (1957).

<sup>13</sup> T. Kinoshita and A. Sirlin, Phys. Rev. **113**, 1652 (1959).

<sup>14</sup> S. M. Berman, Phys. Rev. **112**, 267 (1958).

FIG. 1. A typical picture showing a variety of  $\pi$ - $\mu$ - $e$  decays.



The dependence of the asymmetry on momentum has been measured with counters<sup>23,24,25</sup> and using emulsions.<sup>26</sup> The asymmetry of very low-energy electrons has also been studied using a propane bubble chamber.<sup>27</sup> These experiments have been troubled with poor resolution which prevent them from examining the entire spectrum.

The present experiment is an attempt to measure both the momentum spectrum and the asymmetry spectrum with improved resolution and statistics.

## II. APPARATUS

The construction, operation, and photography of the liquid hydrogen bubble chamber used in this experiment has been described in detail elsewhere.<sup>28</sup> The chamber operated in a stable and trouble-free manner producing tracks of good contrast with no observable distortion when the light was flashed 1 millisecond after the beam

entered the chamber. The density of hydrogen in the expanded chamber was determined from the range of  $\mu$ 's from  $\pi$ - $\mu$  decay to be  $0.0565 \pm 0.0005$  g/cm<sup>3</sup>.

The details of the beam are not relevant to this experiment and will not be discussed except to note that 10-15  $\pi^+$  mesons stopped in a useful region of the chamber in each picture. Muon and electron contamination was of the order of 25%, but was unimportant as  $\pi$ - $\mu$ - $e$  decays from stopped pions were selected for measurement by their characteristic appearance (see Fig. 1) and later checked by the measured length of the muon track. The only possible source of contamination arose from muons that scatter and then decay in flight about 1 cm from the scatter. Of the approximately 10 000 events utilized, one might be expected to follow this pattern and would, of course, produce a negligibly small effect on the results.

20 000 good quality pictures were taken showing about 200 000  $\pi$ - $\mu$ - $e$  decays. 5000 of these pictures were scanned and 19 500 events were measured.

## III. MEASUREMENTS

An event was selected for measurement if it satisfied the following criteria:

1. The  $\mu$  stopping must be inside a circle drawn on clear plastic and lined up with the projected picture by means of fiducial marks on the chamber. This condition guaranteed that the  $\mu$  stopping was at least 2 cm from the cylindrical walls of the chamber and so was in the well-illuminated region of the chamber.

2. The projected length of the muon must be less than half its actual length. This criterion selected preferentially events in which the muon momentum had a large component along the camera axis and so along

36, 1327 (1959) [translation-Soviet Phys.-JETP 36(9), 940 (1959)].

<sup>21</sup> G. R. Lynch, J. Orear, and S. Rosendorff, Phys. Rev. 118 284 (1960).

<sup>22</sup> A. Abashian, R. K. Adair, R. Cook, A. Erwin, J. Kopp, L. Leipuner, T. W. Morris, D. C. Rahm, R. R. Rau, A. M. Thorndike, W. L. Whittemore, and W. J. Willis, Phys. Rev. 105, 1927 (1957).

<sup>23</sup> D. Berley, T. Coffin, R. L. Garwin, L. M. Lederman, and M. Weinrich, Phys. Rev. 106, 835 (1957).

<sup>24</sup> H. Kruger and K. M. Crowe, Phys. Rev. 113, 341 (1959).

<sup>25</sup> J. M. Cassels, T. W. O'Keefe, M. Rigby, and J. Wormald, Proc. Phys. Soc. 72, 781 (1958).

<sup>26</sup> Proceedings of the Ninth Annual High-Energy Physics Conference, Kiev, 1959 (unpublished).

<sup>27</sup> I. A. Pless, A. E. Brenner, R. W. Williams, R. Bizzari, R. H. Hildebrand, R. H. Milburn, A. M. Shapiro, K. Strauch, J. C. Street, and L. A. Young, Phys. Rev. 108, 159 (1957).

<sup>28</sup> F. Eisler, R. Plano, N. Samios, M. Schwartz, and J. Steinberger, Nuovo cimento 5, 1700 (1957).

the magnetic field. Such events preserved a large part of the muon polarization and so were the most useful for the asymmetry spectrum while also being useful for the momentum spectrum.

Once selected, an event was measured immediately. The cartesian coordinates of the following points were determined in each of the three views for each event. 1. Two fiducial marks, to determine the magnification, rotation and translation of the views relative to a standard coordinate system. 2. The  $\pi$ - $\mu$  decay vertex. 3. The  $\mu$ - $e$  decay vertex. 4. Two further points along the electron track roughly equally spaced and at roughly the same points along the track in all three views.

These measurements were made on a digitized scanning machine with a precision corresponding to 0.017 cm in the life-size chamber. Events were measured by nonphysicists at the rate of one every five minutes averaged over an eight-hour day.

#### IV. CALCULATION OF SPACE PROPERTIES

An IBM 650 program was written to find the vector momentum of the electron, the direction of the  $\mu$ , and various space properties used to select events likely to be well measured without biasing the spectra. The calculation of the momentum of the electron is of critical importance to the determination of the  $\rho$  parameter and will be discussed in detail here.

There were four main contributions to the systematic error in the momentum scale: (1) geometrical reconstruction, (2) turbulence, (3) magnetic field, and (4) energy loss.

The measurement error on an individual track was determined to be 1.5% of the momentum for an average track by remeasuring 220 events in the usual manner. This is about  $\frac{1}{4}$  of the average multiple scattering uncertainty and so produced an almost negligible broadening of the resolution function. A systematic error in the momentum arose mainly from the error in knowing the distance between the fiducial marks ( $22.41 \pm 0.01$  cm) and from nonlinearities in the lineup of the scanning machine. These effects were estimated to contribute 0.1% to the systematic error.

To determine the effect of turbulence in the chamber, the deviation of 875 no-field pion tracks from a straight line was measured. These tracks crossed the central region of the chamber horizontally while the expander was on top of the chamber, so it was expected that these tracks would be quite sensitive to turbulence. A histogram of the deviations is shown in Fig. 2. The data is well fit by a Gaussian with standard deviation 0.84 mm and average  $-0.004 \pm 0.028$  mm. This standard deviation would be expected from multiple scattering for a pion energy of 42 Mev, which is in satisfactory agreement with the expected beam energy. The average deviation is clearly consistent with no distortion due to turbulence. Furthermore, since the electron tracks were oriented in a random fashion, to first order such a dis-

tortion would not produce a stretching of the momentum scale. A contribution of 0.1% from turbulence to the systematic error was therefore considered conservative.

The magnetic field was mapped throughout the chamber to an accuracy of 0.1% and fit by a function which was constrained to satisfy Maxwell's equations. The maximum field variation in the useful region of the chamber was less than 400 gauss, about 4% of the central value which was  $8841 \pm 7$  gauss.

To account for the variation in the field along the path of the electron, an effective field was obtained by taking the weighted average of the field at the beginning, middle and end of the track with weights  $\frac{1}{2}$ ,  $\frac{5}{6}$ , and  $\frac{1}{2}$ , respectively. It can easily be shown that this is essentially exact if the track is almost straight and the field is a quadratic function of the coordinates. This is an adequate approximation for our purposes.

The above discussion refers only to the "z" component of the magnetic field. No attempt was made to correct for the radial component of the field as it had a small effect on the curvature of a track—about  $\frac{1}{2}\%$  for an average track—and tends to average out for a large number of randomly oriented tracks.

The momentum must also be corrected for energy loss by ionization. The average correction is about 1.5 Mev/c which is 4% of the average momentum of the spectrum. The energy loss was evaluated experimentally to an accuracy of 2.5% so the resulting uncertainty in the momentum was 0.1%.

The measurement of energy loss utilized electrons which spiraled around many times in the chamber and gave for the average total energy loss between 26 Mev/c and 0,  $dE/dx = 0.224 \pm 0.003$  Mev/cm. The energy dependence of the ionization energy loss was calculated from the theory by Lecourtois<sup>29</sup> as there was no practical method for experimentally determining energy loss at higher energies with the required precision. The result of this calculation was that the ionization loss is constant to within 2% for momenta above 10 Mev/c.

The momentum was also corrected for the average energy lost by radiation. This correction was only about  $\frac{1}{2}\%$  for an average track so this correction had to be

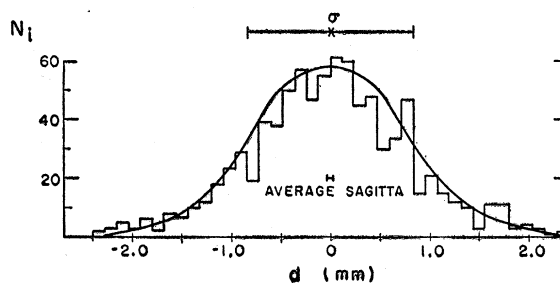


Fig. 2. A histogram of the sagitta of 875 no-field pion tracks used to study possible distortions in the chamber.

<sup>29</sup> Agnes Lecourtois (private communication). I would like to express my thanks to Miss Lecourtois.

known to only 20% to maintain an accuracy of 0.1% in the momentum. For this purpose the simple equation  $(dE/dx)_{\text{rad}} = E/X_0$  was used, where  $E$  is the energy of the particle and  $X_0$  is the radiation length. The radiation length calculated with no screening<sup>30</sup> was 72.5 g/cm<sup>2</sup> = 1300 cm in this chamber. The average momentum of the electrons used to measure the energy loss was 11.8 Mev/c, so the average energy loss due to ionization and radiation was  $(dE/dx)_{\text{tot}} = 0.224 + 0.00077(p - 11.8) = 0.215 + 0.00077p$  Mev/cm.

This was used to correct the momentum for energy loss by adding to the momentum the energy lost in half the track length measured plus a small term which depended on the position of the middle measured point. The form of this correction was checked and shown to be accurate to better than 0.1% for an average track assuming the path of the electron to be a logarithmic spiral. This would be exactly true if the energy loss were constant and if there were no multiple scattering.

The systematic error in the momentum scale was due to these four independent effects and amounted to 0.2%.

## V. MOMENTUM SPECTRUM

### A. Selection of Events

The validity of this or any similar experiment depends on an accurate evaluation of the systematic errors. In this experiment, the main contributions to the systematic error came from possible stretching of the momentum scale, which was discussed in the previous section, and from possible biases in the selection of events.

The criteria used to select events from the sample of measured events for use in the momentum spectrum were chosen to keep the sample as large as possible and to be independent of momentum while eliminating most events which could be measured only very poorly. For these purposes, the following selection criteria were used:

1. The dip angle of the track must be less than 45°.
2. The potential path of the track must be greater than 7 cm. The potential path is the distance from the decay vertex to the nearest wall of the chamber along the initial direction of the electron.
3. Events for which the  $\mu$ -e decay vertex was within one cm of either glass wall were not used.
4. Events for which measurements made in the three views were grossly inconsistent were discarded. This criterion was set at 15 standard deviations and rejected less than  $\frac{1}{2}\%$  of the events.

9213 of the 19 500 events measured satisfied these criteria and were used in the determination of the  $\rho$  parameter. A histogram of these events is shown in Fig. 3.

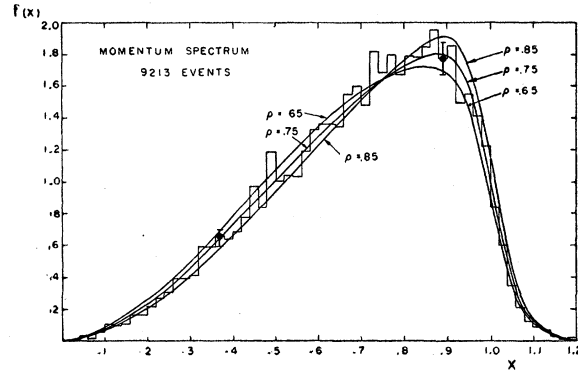


FIG. 3. A histogram of the data used to evaluate  $\rho$ . The error flags are representative statistical errors. Also shown are the theoretical spectra for three  $\rho$  values with the resolution folded in.

### B. Resolution Function

In order to compare the data with the theory and extract a  $\rho$  value, it was necessary to fold into the theoretical spectrum the resolution function which described the distortion of the spectrum due to the finite precision of measurement. Three effects contributed appreciably to the resolution width in this experiment: (1) external radiation, (2) ionization loss straggling, and (3) measurement and multiple scattering.

The first step was to calculate the theoretical spectrum including the internal radiative corrections. This was done using Eq. (1) with the small term proportional to  $\eta$  neglected. The Michel spectrum then assumes the simple form:

$$P(x) = [1 + h(x)] \{12x^2 - 12x^3 + \rho[(32/3)x^3 - 8x^2]\}. \quad (2)$$

A mesh 0.01 wide in  $x$  was used in this calculation and the values of  $h(x)$  which describe the internal radiative corrections were taken from reference 17, which tabulates  $h(x)$  averaged over  $x$  intervals of various widths. The values of  $h(x)$  averaged over the interval  $\Delta x = 1m_e = 0.0097$  were used here. These tables contain the latest values for the internal radiative corrections and are now agreed upon by several authors.<sup>13,14</sup>

The momentum of each electron was corrected for the average energy lost due to radiation while passing through the liquid hydrogen. However, an individual electron could lose any fraction of its energy. Therefore, to obtain the correct shape for the Michel spectrum, a bremsstrahlung spectrum was folded in.<sup>31</sup> This has the form:

$$w(k) = \frac{l}{X_0} \frac{dk}{k} \cong 0.005 \frac{dk}{k}. \quad (3)$$

Here  $l$  is half the length of the average track (6.5 cm),  $X_0$  is the radiation length for fast electrons in liquid hydrogen (1300 cm), and  $k$  is the energy of the proton

<sup>30</sup> E. Segrè, *Experimental Nuclear Physics* (John Wiley & Sons, New York, 1953), Vol. I.

<sup>31</sup> W. Heitler, *The Quantum Theory of Radiation* (Oxford University Press, New York, 1954), 3rd ed.

emitted. This was folded into the theoretical spectrum using a mesh width of 0.002 in  $x$ .

The momentum of each electron was also corrected for the average energy lost due to ionization. However, there was straggling about the average energy loss which for this experiment had a full width at half maximum of 0.2 Mev. To correct for this effect, the Landau straggling distribution was used. This has been checked experimentally,<sup>32</sup> giving good agreement with the theory for light elements. Since, in this experiment, electrons with delta rays of greater than 4 Mev were measured only up to the delta ray, the straggling function was extended out to 4 Mev above the most probable energy loss using Landau's inverse-square behavior for this region. For this calculation, a mesh 0.002 wide in  $x$  was used.

By far the largest contribution to the width of the over-all resolution function came from the finite precision of measurement (1.5%), and the intrinsic uncertainty in measuring the momentum of a particle due to multiple scattering in the liquid hydrogen (6%). Both these effects lead to a resolution function of the same type and will be considered together.

To determine the momentum of an electron, the radius of curvature of the track was found by measuring three roughly equally spaced points along the track. For the purposes of the error analysis, the following approximate relationship is useful.

$$R = l^2/8d. \quad (4)$$

Here  $R$  is the radius of the track,  $l$  is the chord length between the ends of the track, and  $d$  is the sagitta—the distance along a perpendicular to the chord from the midpoint of the chord to the track. Since, for the average track,  $d$  was 1 cm and  $l$  was 13 cm, the error in  $R$  was due mainly to the uncertainty in  $d$ . The error in  $d$  due to measurement was clearly Gaussian distributed. Multiple scattering also produces a Gaussian distribution in the sagitta to a good approximation as is indicated by Fig. 2. These two effects can thus be combined into a single Gaussian.

The standard deviation due to measurement was estimated to be 0.017 cm by an analysis of 220 remeasured events. The standard deviation due to multiple scattering was calculated using the method first discussed by Bethe<sup>33</sup> with the result:

$$\sigma_{ms} = \frac{2.16}{p\beta} \frac{l^{\frac{3}{2}}}{\sqrt{X_0}}. \quad (5)$$

Here  $l$  is the length of the track in space in cm,  $p$  is the momentum of the particle in Mev/c,  $\beta$  is the speed of the particle, and  $X_0$  is the radiation length in cm.

The probability distribution in momentum assuming

a Gaussian distribution in the sagitta was then obtained by the standard method.

$$R_\sigma(x, y) = \frac{1}{(2\pi)^{\frac{1}{2}} \sigma} \frac{x}{y^2} \exp \left\{ -\frac{[(y-x)/y]^2}{2\sigma^2} \right\},$$

$$\sigma = \frac{1}{l^2 \cos \alpha} (C_1 x^2 + C_2 l^3)^{\frac{1}{2}}, \quad (6)$$

$$C_1 = \left( \frac{26.7 p_{\max} \sigma_{\text{meas}}}{H} \right)^2, \quad C_2 = \frac{3.33 \times 10^3}{H X_0}.$$

This function  $R_\sigma(x, y)$  is the probability that an electron emitted at momentum  $x$  was measured to have momentum  $y$  due to the measurement and multiple scattering uncertainties. Here  $\alpha$  is the angle between the track and the chamber midplane—the dip angle—and the other symbols have been defined.

This function is quite close to a Gaussian for small  $\sigma$ , but the most probable momentum is decreased slightly and the average momentum is increased by roughly  $\sigma^2$ . Since the width of this resolution function is proportional to  $\sigma$  while the effect on the average momentum is proportional to  $\sigma^2$  and because the sum of several Gaussians with different widths is not a Gaussian, it was not possible to make an accurate representation of the actual resolution function using a single width. The measurement and multiple scattering resolution function was therefore taken to be the weighted sum of 9 individual resolution functions  $R_\sigma(x, y)$  weighted with the probability of each  $\sigma$  as determined from a histogram of the  $\sigma$ 's calculated for all events used in the spectrum. This was then folded into the spectrum resulting from the two previous folding operations using a mesh width of 0.006 in  $x$  to obtain the theoretical spectrum with all resolution folded in for comparison with the data.

### C. Statistical Analysis

The comparison of the data with the theoretical spectra was carried out using the least mean squares method.<sup>34</sup> This method consists in evaluating the  $\chi^2$  function:

$$\chi^2 = \sum [(F_i - N_i)/\sigma_i]^2. \quad (7)$$

Here  $N_i$  is the number of events in the  $i$ th interval which was chosen to be 0.01 wide in  $x$ ,  $F_i$  is the theoretical spectrum normalized to the total number of events used and evaluated at the center of the  $i$ th interval. It is a function of the  $\rho$  parameter and any other parameters to be evaluated from the data.  $\sigma_i$  is the expected error and was set equal to  $\sqrt{F_i}$ . The sum is extended over the entire spectrum. Intervals with fewer than 10 events were lumped together with neighboring intervals until at least 10 events were grouped together.

<sup>32</sup> E. L. Goldwasser, F. E. Mills, and A. O. Hanson, Phys. Rev. 88, 1137 (1952).

<sup>33</sup> H. Bethe, Phys. Rev. 70, 821 (1946).

<sup>34</sup> Harold Cramer, *The Elements of Probability Theory* (John Wiley & Sons, New York, 1955).

The dependence of  $\chi^2$  on  $\rho$ , assuming the systematics were exactly correct, is shown by the central parabola of Fig. 4. The best fit was obtained for  $\rho = 0.780 \pm 0.016$ , where the error is statistical only. The systematic error in the momentum scale has been estimated to be 0.2%, due to measurement error plus an additional 0.1% for a possible selection bias for a total systematic error of 0.23%. The dependence of  $\rho$  on a stretching of the momentum scale can be easily estimated by evaluating  $\rho$  as a function of the average momentum of the spectrum. Ignoring internal radiative corrections and the resolution function:

$$\rho = 7.5(\bar{x} - 0.6). \quad (8)$$

Since  $\bar{x} \sim 0.7$  for  $\rho \sim 0.75$ ,

$$\delta\rho \sim 5\delta\bar{x}/\bar{x}, \quad (9)$$

and systematic errors contribute 0.012 to the error in  $\rho$ . Adding this in quadrature,  $\rho = 0.780 \pm 0.020$ .

Since  $\rho$  is quite sensitive to systematic errors in the momentum scale and since the data contain information about the momentum scale—particularly from the position of the end point— $\chi^2$  was also evaluated as a function of a stretching of the momentum scale by  $\Delta\%$ . Finally,  $\chi^2$  was evaluated as a function of the average width of the measurement and multiple scattering resolution function to check that calculation and to find the sensitivity of  $\rho$  to an error in the resolution width. The result of this many parameter fit to the data was

$$\begin{aligned} \Delta &= +0.0025 \pm 0.0037, \quad \bar{\sigma} = 0.058 \pm 0.003, \\ \rho &= 0.792 \pm 0.024. \end{aligned}$$

These errors all include correlations due to uncertainties in the other parameters. Therefore, this is the  $\rho$  value and error which would have been obtained if no attempt had been made to calibrate the momentum scale or determine the average width of the resolution function. This result depends appreciably only on the momentum scale being linear. The fact that  $\Delta$  is consistent with zero within the error indicates that no large error was made in the calibration of the momentum scale.

A detailed examination of this calculation showed that  $\rho$  is essentially uncorrelated with  $\bar{\sigma}$ , but is strongly correlated with  $\Delta$  in a manner given with good precision

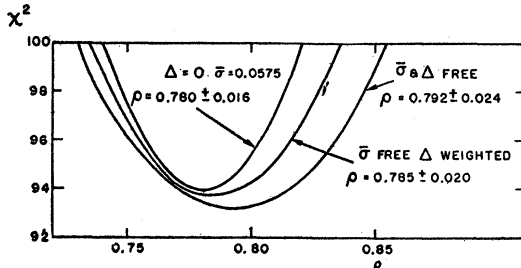


FIG. 4.  $\chi^2$  determination of  $\rho$  showing the effect of correlations with  $\bar{\sigma}$  and  $\Delta$ .

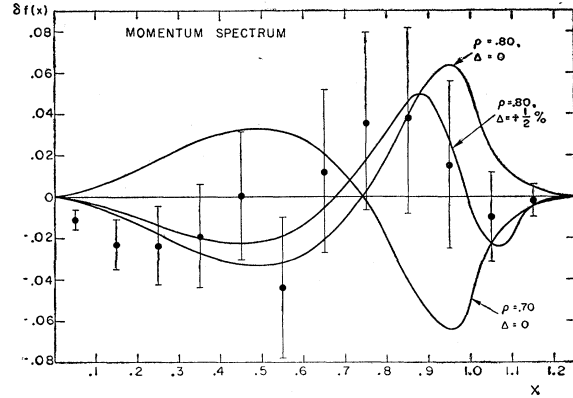


FIG. 5. The deviation of the data and theoretical spectra with resolution folded in from the theoretical spectrum for  $\rho = \frac{3}{4}$ ,  $\Delta = 0$ .

by Eq. (9). As the momentum scale was calibrated (with a precision of 0.23%) as discussed in Sec. IV, this measurement was added to the  $\chi^2$  function to obtain the final result  $\rho = 0.785 \pm 0.020$ , where the error now contains the contribution due to systematic errors.

The minimum  $\chi^2$  obtained was 93.8, which is to be compared with the  $99 \pm 14$  expected for 99 degrees of freedom. The fit is somewhat better than expected, but well within the predicted limits.

In order to make the goodness of fit and the sensitivity of the data in determining  $\rho$  more apparent, Fig. 5 was drawn. This figure shows the deviations of the data and the theoretical spectra from the theoretical spectrum for  $\rho = 0.75$ ,  $\Delta = 0$ ,  $\bar{\sigma} = 0.0575$ . This makes it possible to expand the scale so the differences between spectra for different values of  $\rho$  become more apparent. To improve the statistics on each point, the data was summed over intervals 0.1 wide in  $x$  instead of 0.02 as in Fig. 3. It is clear that the best values for  $\rho$  and  $\Delta$  ( $\rho = 0.785$ ,  $\Delta = +\frac{1}{8}\%$ ) represent a good fit and that  $\rho = 0.75$  is a poorer fit to the majority of points. The only region where the fit to  $\rho = 0.785$  is noticeably bad is at  $x < 0.2$ . It is believed that there was no bias against these low-energy electrons as an electron with a momentum as low as  $x = 0.01$  was easily seen and measured. With 10 000 events in the entire spectrum, only about 7 were expected in the region  $x < 0.05$  and 4 were found. At any rate, a rough calculation showed that 25 events, in addition to the 143 found in the region  $x < 0.2$ , would produce an excellent fit and would alter  $\rho$  by less than 0.007. Since this discrepancy could well be a statistical fluctuation, no correction was made.

An attempt to evaluate the second Michel parameter  $\eta$  was strongly affected by this apparent shortage of low-energy electrons. A least mean squares fit to  $\rho$  and  $\eta$  gave  $\eta = -2.0 \pm 0.9$ ,  $\rho = 0.745 \pm 0.025$ . Since  $\eta$  is restricted by its definition to  $-1 \leq \eta \leq +1$ , and because of the large error, this fit shows little more than that  $\eta$  cannot be determined from this data. The large negative value is due entirely to the apparent lack of events at low energy. The effect on  $\rho$  is more disturbing. How-

ever,  $\eta$  is restricted to  $|\eta| \leq 0.44$  by its relation to the asymmetry parameter  $|\eta|^2 \leq 1 - |\xi|^2$  and the experimental result  $|\xi| \geq 0.92$ .<sup>18</sup> If the coupling is  $V-A$ ,  $\eta=0$ . Restricting  $\eta$  to  $|\eta| < 0.44$  would reduce its effect on  $\rho$  to 0.009. Because of this and several other small but difficult to evaluate possible contributions to the systematic error, an additional error of 0.015 was added in quadrature to obtain for the error 0.025.

As a check on the selection criteria and the measurement of dipping tracks; those events which had a dip angle less than  $23.6^\circ$ , a potential path greater than 10 cm and satisfied the other old selection criteria, were analyzed. The resulting 4581 events gave a  $\rho$  value of  $0.780 \pm 0.035$  in good agreement with the "poor" resolution result.

A small bias against low-momentum electrons was introduced by the selection criteria because a muon which decayed near a glass window was more likely to be polarized with its spin pointing away from the glass. This occurred because most pions stopped in the central region of the chamber. The low-momentum electrons were then preferentially emitted in the direction of the glass as predicted by the asymmetry spectrum and were less likely to have a potential path greater than 7 cm than a high-momentum electron. This effect is easily and accurately calculable using the observed distribution of stopping pions, and the shape of the momentum and asymmetry spectra [Eq. (1)]. The result of this correction is to reduce the  $\rho$  value by 0.005 to 0.780.

The final result is then  $\rho = 0.780 \pm 0.025$ .

## VI. ASYMMETRY SPECTRUM

### A. Selection of Events

Events were selected for inclusion in the asymmetry spectrum by a set of criteria designed to be independent of the electron momentum and direction while tending to reject events which could be measured only poorly. However, since the statistical error is the dominant error in the asymmetry parameters in this experiment,

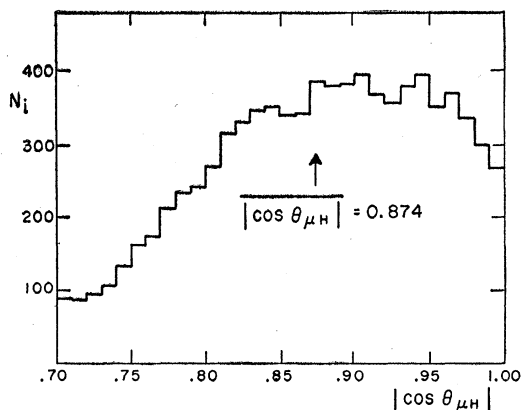


FIG. 6. Histogram of the absolute value of the cosine of the angle between the magnetic field and the  $\mu$ -meson momentum for the events used in the asymmetry spectrum (8354 events).

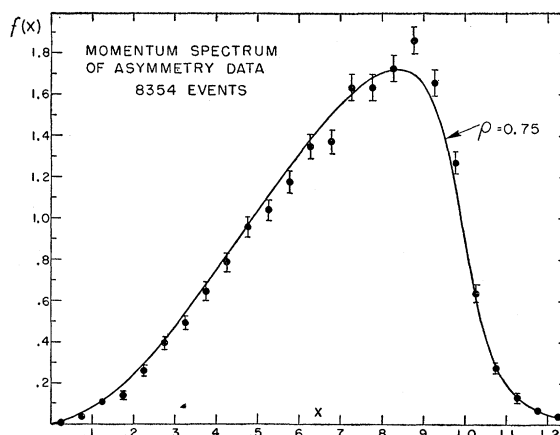


FIG. 7. The momentum spectrum of the events used in the asymmetry spectrum. Also shown is the theoretical spectrum for  $\rho=0.75$  with the resolution function expected for these events folded in.

the criteria were made considerably less stringent than those used for the momentum spectrum. The criteria used were:

1. The length of the muon must be between 1.0 and 1.3 cm. The average muon length was  $1.149 \pm 0.001$  cm.
2. The redundancy from measuring the coordinates in three views was again used to eliminate events in which very large measurement errors were made.
3. The  $\mu$ - $e$  decay vertex must be at least 3 cm from the windows of the chamber.
4. A second type of potential path,  $L_{p2}$ , was defined to be zero if the  $\mu$ - $e$  decay vertex was more than 13 cm from the center of the chamber (the radius of the chamber was 15 cm) and otherwise to be the distance from the  $\mu$ - $e$  decay vertex along the projection of the initial direction of the electron in the chamber plane to a cylinder of radius 13 cm concentric with the chamber. Events with  $L_{p2}$  less than 3 cm were not used.
5. Events for which the dip angle of the electron was more than  $72^\circ$  were not used.
6. The absolute value of the cosine of the angle between the muon and the magnetic field must be greater than 0.7.

The last criterion selected those events in which the polarization of the muon at decay was at least 70% of its polarization at emission, assuming the muon was polarized in the direction of its momentum and that it was not depolarized by the liquid hydrogen. The average polarization of the sample of muons used was then simply given by the average of the absolute value of the cosine of the angle between the muon momentum and the magnetic field. The distribution obtained is shown in Fig. 6 and gave for the average polarization  $\bar{P} = 0.874$ .

The momentum spectrum of the events used in the asymmetry spectrum is shown in Fig. 7. The expected distribution for  $\rho=0.75$  with the resolution function

expected for these events folded in is also shown. The main purpose of this graph is to check the selection criteria and the resolution function, but it can be seen that the agreement of the data with  $\rho=0.75$  is quite good though favoring a somewhat higher  $\rho$  value.

The asymmetry spectrum was calculated from the data in the standard way using the average of  $\cos\theta$ , where  $\theta$  is the angle between the electron momentum and the polarization vector (taken to be the component of the  $\mu$  momentum along the magnetic field with the algebraic sign changed). This was done for momentum intervals  $\Delta x=0.05$  throughout the spectrum to obtain the momentum dependence of the asymmetry. The expression used was:

$$g_\delta(x) = \frac{3\langle(\cos\theta)_i\rangle_{\text{av}} N_i}{(0.95)^3 P N \Delta x} \pm \frac{1}{0.95 \bar{P} N \Delta x} (3N_i)^{1/2}. \quad (10)$$

Here  $\theta$  is the angle defined above,  $N_i$  is the number of events in the  $i$ th momentum interval,  $\bar{P}$  is the average polarization, and  $N$  is the total number of events in the spectrum. The 0.95 factor enters because only electrons with  $|\cos\theta| < 0.95$  were used in the spectrum. (See asymmetry selection criterion 5.) The data with their statistical errors are shown in Fig. 8.

### B. Resolution Function

The resolution function was treated in the same manner as for the momentum spectrum. The major difference arose from the fact that the measurement and multiple scattering widths were larger here because more poorly measured events were included in this spectrum than in the momentum spectrum. This situation was intensified as tracks with large dip angles carry the most information about the asymmetry and these tracks were the ones measured most poorly. This effect was included in the resolution function. The resulting resolution function had a standard deviation of about 9%.

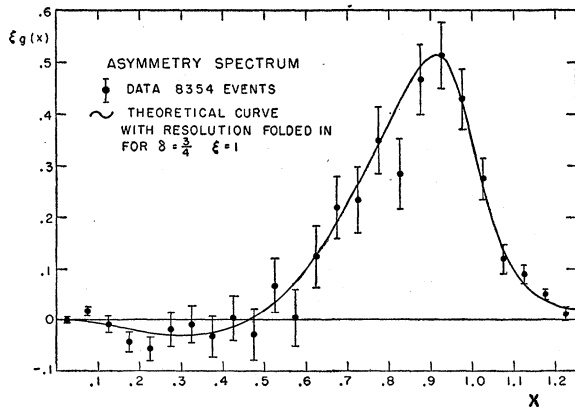


FIG. 8. The asymmetry spectrum. The error flags represent the data and the smooth curve is the theoretical spectrum for  $\delta=3/4$ ,  $\xi=1$ , with resolution folded in.

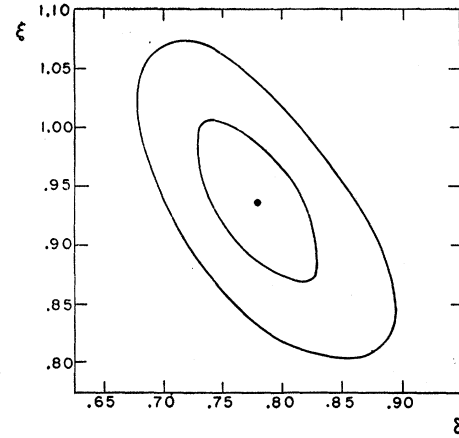


FIG. 9.  $\chi^2$  determination of the asymmetry parameters  $\xi$  and  $\delta$  showing the correlation between the two parameters.

### C. Statistical Analysis

The evaluation of the parameters  $\xi$  and  $\delta$  with their errors from the data was done by a least mean squares calculation similar to that used to analyze the momentum spectrum. The results of this calculation are shown in Fig. 9. The central point gives the values of  $\xi$  and  $\delta$  for which  $\chi^2$  is a minimum and represents the best fit to the data. The inner error ellipse gives all values of  $\xi$  and  $\delta$  for which  $\chi^2$  is one above its minimum value and corresponds to one standard deviation; on the outer ellipse  $\chi^2$  is four above its minimum value. Since the ellipses lie at an angle to the axes, the two parameters are correlated as expected.

The minimum  $\chi^2$  obtained was 18.7 and the number of degrees of freedom was 23. The chance of the fit being this bad or worse according to the  $\chi^2$  distribution<sup>21</sup> is about 70%. This means that the fit is somewhat better than expected, but would be still better in 30% of such experiments.

The result of this analysis is  $\delta=0.78\pm0.05$ ,  $|\xi|=0.94\pm0.07$ . The errors given are statistical only as the systematic errors are negligibly small. For example, the 0.23% uncertainty in the calibration of the momentum scale would generate an error of 0.006 in  $\delta$  and leave  $\xi$  essentially unchanged.

Since the two parameters are correlated, assuming a fixed value for either will alter the result obtained for the other. For example, two-component theory specifies  $\delta=0.75$  and leaves  $\xi$  free. Assuming  $\delta=0.75$ , as has been done in most measurements of  $\xi$ ,<sup>3,4,18-22</sup> this experiment gives  $|\xi|=0.96\pm0.05$ .

### VII. CONCLUSIONS

The results of this experiment— $\rho=0.780\pm0.025$ ,  $\delta=0.78\pm0.05$ ,  $|\xi|=0.94\pm0.07$ —can be compared with two component theory and with the “universal”  $V-A$  theory both of which predict  $\rho=0.75$ ,  $\delta=0.75$ . If the coupling is  $V-A$ , violation of conservation of parity is a



maximum and  $|\xi|=1$ . It is concluded that these data are adequately fit by  $V$ - $A$  theory.

### VIII. ACKNOWLEDGMENTS

The author would like to express his gratitude to Professor Jack Steinberger for many helpful and stimulating discussions, and for his active assistance. The aid of a number of other people with various phases of the experiment is deeply appreciated. The author would especially like to thank Dr. Daniel Tycko for help with

programming the IBM 650, Dr. Edgar Jenkins for the magnetic field measurements, Dr. Gerhard Fischer for the ionization loss measurement, Dr. Agnes Lecourtous for her calculation of the ionization loss, Mrs. Dina Goursky, Mrs. Anne Osgood, and Alex Woskry for their patient and painstaking scanning and measurements of events, and Miss Catherine Macleod for her help in keeping almost 100 000 IBM cards and other records in good order.

## Anelasticity of $p$ - $p$ Collisions at 2.7 Bev\*†

W. M. BUGG AND D. T. KING  
The University of Tennessee, Knoxville, Tennessee  
(Received April 11, 1960)

By following the tracks of particles in a direction generally contrary to that of the incident 2.7-Bev proton beam, a series of observations interpreted as  $p$ - $p$  collisions has been made in nuclear emulsions. The angular and momentum distributions of particles outgoing from these interactions, and hence the relative occurrence of  $p$ - $p$  collisions with different pion multiplicities, are in reasonable accord with foregoing work. An attempt is made to distinguish triple pion production processes from those of double production. Even though the c.m. kinetic energy distributions for the respective production modes are markedly different, the corresponding anelasticity characteristics show a general similarity.

### INTRODUCTION

AS observations of increasingly energetic collisions between fundamental particles become possible, it is of interest to examine the concept of collision anelasticity. This appears as a variable quantity in Heisenberg's theory of multiple pion production in nucleon-nucleon interactions.<sup>1</sup> A number of determinations of this quantity has been made on cosmic-ray jets, under some far-reaching assumptions.<sup>2</sup> Direct determination of the anelasticity is only possible when the interaction results in the creation of particles with characteristics clearly distinguishable from those of the primary particles. Then, even if charge exchange occurs, the anelasticity may be defined as the fraction of the available energy in the center-of-mass system of the colliding particles that is carried away by the created particles. When one or more of the created particles is indistinguishable from one of the primaries, it is still possible to test a prediction of the anelasticity characteristic. This is done by designating the created particles in accordance with a convenient rule, and computing the effect of this rule in distorting the theoretical anelasticity characteristic. By this means it has been shown that in the direct

creation of an electron pair by a fast electron, the fractional energy loss of the primary to the created pair is satisfactorily predicted by the theory.<sup>3</sup> For those interactions for which the initial particles are not among the products, the term anelasticity must be redefined.

In this study we have determined the anelasticity of a number of proton-proton collisions in emulsion at 2.7 Bev. The measurements were confined to interactions from which at least two charged pions emerged. This enables a comparison of double and triple pion production at an energy for which quadruple production is negligible,<sup>4</sup> yet derived from about 40% of all proton-proton interactions.<sup>4-6</sup> With some exceptions, the determination of anelasticity for collisions in which two charged pions are produced must be regarded as a lower limit of a possible triple pion production process in which the third, neutral, pion escapes undetected.

The nucleon isobar theory has had considerable success in the interpretation of single pion production processes by nucleons,<sup>7</sup> pions,<sup>8</sup> and photons<sup>9</sup> of energies up to about 1 Bev. A prediction of the c.m. kinetic energy distribution of the pions arising from double production

\* This work was supported by a grant from the National Science Foundation.

† This paper is based on a thesis submitted by W. M. Bugg to the Graduate School of The University of Tennessee in partial fulfillment of the requirements for a Ph.D. degree.

<sup>1</sup> W. Heisenberg, *Z. Physik* **126**, 569 (1949).

<sup>2</sup> T. F. Hoang, *J. phys. radium* **15**, 337 (1954).

<sup>3</sup> M. M. Block, D. T. King, and W. W. Wada, *Phys. Rev.* **96**, 1627 (1954).

<sup>4</sup> M. M. Block *et al.*, *Phys. Rev.* **103**, 1484 (1956).

<sup>5</sup> R. Cester, T. F. Hoang, and A. Kernan, *Phys. Rev.* **103**, 1443 (1956).

<sup>6</sup> W. M. Bugg, doctoral dissertation, 1959 (unpublished).

<sup>7</sup> A. P. Batson *et al.*, *Proc. Roy. Soc. (London)* **251**, 218 (1959).

<sup>8</sup> W. D. Walker and J. Crussard, *Phys. Rev.* **98**, 1416 (1955).

<sup>9</sup> J. M. Sellen *et al.*, *Phys. Rev.* **113**, 1323 (1959).